1

Introduction

TABLE OF CONTENTS

1.1 Theoretical and Computational Chemistry

Theoretical and computational chemistry, a vibrant nexus of chemical disciplines, seamlessly melds chemical principles with the rigor of physics, the intricacy of biology, and the power of computer science. Through sophisticated mathematical models, fundamental physical laws, and cutting-edge computational techniques, this subdiscipline of chemistry delves into the electronic-structure realm of matter, simulating complex chemical processes, predicting physicochemical properties, and unlocking profound insights into molecules, biological systems, and materials.

The evolution of modern theoretical and computational chemistry traces back to the early twentieth century with the advent of quantum physics. Trailblazers like Heitler and London [1] pioneered the application of quantum mechanical principles to chemical systems, beginning with the hydrogen molecule H_2, by establishing valence bond theory (VBT) [2–4]. The 1940s marked a turning point as electronic computers, notably ENIAC, enabled rudimentary quantum chemical calculations and transformed theoretical chemistry from a domain of applied mathematics to computational exploration.

In the 1950s and 1960s, the field advanced significantly with the development of ab initio methods within the framework of molecular orbital theory (MOT) [5–7],

such as Hartree–Fock (HR) and post-Hartree–Fock approaches, alongside semi-empirical techniques, facilitating more precise modeling of molecular electronic structures. The 1970s and 1990s introduced density functional theory (DFT) [8–10], parallel computing, and multiscale modeling techniques [11, 12], enabling the study of increasingly complex molecular systems.

By the 2000s, high-performance computing had further expanded the field's capabilities, providing profound insights into chemical reactions, material properties, and atomistic interactions. The early 2010s ushered in the integration of machine learning (ML) techniques, which has been revolutionizing predictive and analytical approaches in computational chemistry [13–15]. Most recently, developments since the early 2020s have centered on quantum computers, artificial intelligence (AI), and deep learning, beginning a new era of unparalleled computational power and precision in molecular modeling [16–19].

Theoretical and computational chemistry encompasses a diverse range of physical methodologies, integrating quantum mechanics (QM), classical mechanics or molecular mechanics (MM), and statistical mechanics to simulate complex systems through advanced multiscale modeling approaches. The recent three Nobel Prizes in Chemistry awarded to the field—John Pople and Walter Kohn in 1998; Martin Karplus, Michael Levitt, and Arieh Warshel in 2013; and David Baker, Demis Hassabis, and John Jumper in 2024—underscore the pivotal role of theoretical and computational chemistry as a cornerstone of interdisciplinary research. This indispensable tool empowers academia and industry alike to unravel complex chemical behaviors, design innovative materials, and explore biological functions with precision and depth.

We cannot just compute; we should also understand [20, 21]. The true value of theoretical and computational chemistry lies not only in generating data but in interpreting it through the lens of chemical concepts. Computational results serve as a bridge between abstract models and real-world phenomena, offering insights that deepen our understanding of molecular behavior, reaction mechanisms, and material properties. However, without a strong grasp of underlying chemical principles, the interpretation of numerical results risks becoming superficial or misleading. Chemical concepts provide the framework for translating numerical output into meaningful knowledge that can guide experiments, predict outcomes, and inspire innovation. Better understanding of chemical concepts through theory and computation fosters the ability to critically evaluate computational predictions, identify limitations, and refine methodologies, ensuring that our models remain robust, reliable, and truly impactful. In this context, Charles Coulson's seminal statement that "we want insight, not numbers" [22, 23] can be nuanced to "we want insight, not *just* numbers," acknowledging that numerical data and deep understanding can work hand in hand.

In this chapter, we will briefly introduce multiscale modeling, followed by three frameworks to solve the Schrödinger equation, VBT, MOT, and DFT, together with the insights from the first two theories, which are both orbital-based, in enhancing our understanding. We will spend a lot more space on the insight from DFT in the ensuing chapters, as it constitutes the central theme of this book.

1.2 Multiscale Modeling

Multiscale modeling [11, 12] is a computational approach that combines systems at multiple spatial and temporal scales to simulate structure, dynamics, reactivity, and functions for complex systems with unprecedented accuracy and detail (Figure 1.1). By bridging the gap between macroscopic observations and microscopic interactions, multiscale modeling enables us to gain insights into systems that cannot be fully understood using a single-scale approach. Multiscale modeling has been well developed as an integral method in theoretical and computational chemistry. The Nobel Prize of Chemistry in 2013 with the citation "*for the development of multiscale models for complex chemical systems*" confirmed just that.

Three key features of multiscale modeling distinguish it from others. (i) It incorporates different simulation models for different spatial scales, from the atomic level (angstrom scale using QM), the mesoscopic level (nanometer scale using classical mechanics), to the macroscopic scale (meter scale using finite element methods). (ii) It couples different models at different scales through mathematical relationships or numerical techniques to pass information from smaller to larger scales; (iii) It is often a hierarchical and bottom-up approach, where one starts at the smallest scale (e.g., atomic or quantum) and builds up to larger scales by averaging or coarse-graining.

At the microscopic scale, which spans from Angstroms and nanometers, simulation methodologies are dominantly QM by solving the Schrödinger equation to describe the electronic structure of molecules and condensed phase materials. MM and molecular dynamics to simulate atomistic motions using Newton's law via classical force fields, and Monte Carlo approaches, which employ stochastic statistics to investigate thermodynamic and kinetic properties, can also be employed. At the mesoscopic level (from nanometers to micrometers), coarse-grained models simplify atomistic details by grouping atoms and functional groups into "beads"

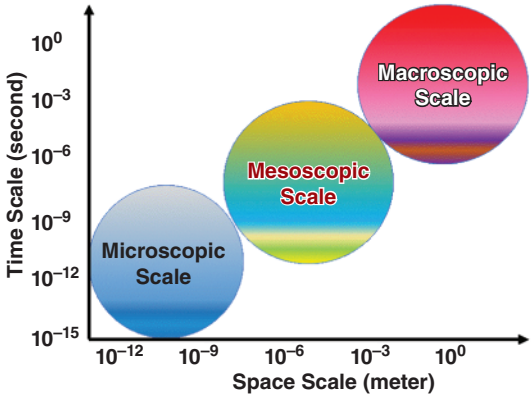

Figure 1.1 Schematic representation of multiscale modeling with respect to time and space scales. *Source*: Reproduced from Ref. [20] with permission of American Chemical Society.

(e.g., via Martini force field or dissipative particle dynamics) to study emergent structural and dynamical behaviors for colloids, polymers, or cellular systems. At the macroscopic level (millimeters to meters and beyond), finite element analysis, fluid dynamics, and continuum mechanics models are applied to study stress, strain, heat transfer, and other macroscopic properties and behaviors for materials.

Depending on the coupling scheme among different scales, which can be sequential, concurrent, and hybrid, we might have different implementations in various disciplines. In computational chemistry, combining quantum mechanical calculations for the region of interest with MM for the rest, that is, QM/MM, is the most popular implementation [24, 25]. QM is applied to describe the part of the system where electronic-level details are crucial, whereas MM is employed to simulate the rest of the system as the environment, for which QM treatment is computationally too costly. One excellent example of such systems is enzymes, because their function spans multiple scales, from electronic interactions at the active site to the dynamics of protein folding and interactions with their environment. For these systems, reactions at the active site are treated quantum mechanically, but for the rest of the enzyme, classical mechanics treatment is adequate. This way of multiscale treatment allows us to simulate enzymatic reaction mechanisms, dynamics, and their roles in biological systems.

While multiscale modeling methods are well established in theoretical and computational chemistry, it still faces multiple challenges. Accurately transferring information between scales is nontrivial, particularly when scales exhibit different behaviors (e.g., discrete atomic interactions versus continuum mechanics). Developing coupling models at different scales can be challenging; large-scale simulations can be computationally expensive, necessitating efficient algorithms and high-performance computing; multiscale models must be parametrized and validated against experimental data at different scales, and any discrepancies in one scale can propagate and impact the results for other scales; Access to accurate and reliable data at all scales is often limited. Meanwhile, harnessing chemical understanding from different scales of simulations is not trivial. Figure 1.2 summarizes the two challenging tasks, computation and understanding, in multiscale modeling. We will come back to this big picture in the last chapter of this book.

In what follows, we focus on solving the Schrödinger equation, which is the foundation of QM governing the electronic structure of matter at the atomic and subatomic level. Without losing generality and unless it is specified otherwise, we consider its time-independent and closed-shell form,

$$H\Psi = E\Psi \tag{1.1}$$

where H represents the Hamiltonian operator, $\Psi \equiv \Psi(\mathbf{r}_1,\mathbf{r}_2,\ldots,\ \mathbf{r}_N)$ denotes the N-electron total wavefunction, and E is the total energy of the many-electron system. For a given system, H is explicitly known, and E can be evaluated by the following expectation value,

$$E = \langle\Psi|H|\Psi\rangle/\langle\Psi|\Psi\rangle \tag{1.2}$$

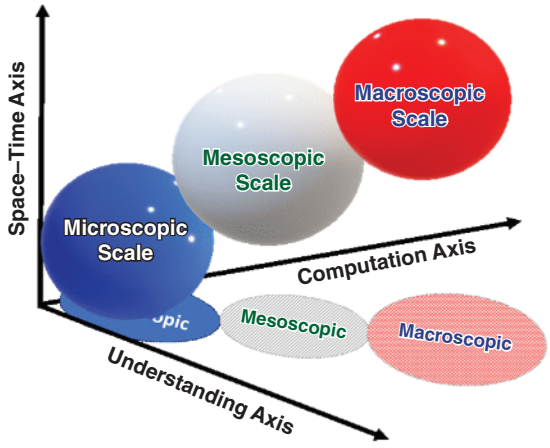

Figure 1.2 Schematic representation of computation and understanding as two paramount and challenging tasks in multiscale modeling. *Source*: Reproduced from Ref. [20] with permission of American Chemical Society.

so in principle there is only one unknown in Eq. (1.1), for example, Ψ. Unfortunately, for a system with N electrons, Ψ is too complicated a function, with $4N$ ($3N$ spatial + N spin) variables. Except for the one-electron case, such as a hydrogen atom or a hydrogen molecular cation H_2^+, only approximate solutions of Ψ are possible. Among the three theoretical frameworks in the literature to approximately solve the Schrödinger equation, that is, VBT, MOT, and DFT, the first two are orbital-based, and the last is density-based. In orbital-based theories, each electron is assumed to be described by an individual wavefunction called an orbital, and the many-electron wavefunction Ψ constitutes a proper combination of the atomic orbital (AO) and/or molecular orbital (MO). In the next section, we quickly overview these two orbital-based theories together with the chemical insights derived from them.

1.3 Orbital-based Theories

1.3.1 Valence Bond Theory

Introduced in the 1920s by Walter Heitler and Fritz London [1] and later refined by Linus Pauling [26], who introduced hybridization and resonance, VBT offers the first framework to approximate the many-electron wavefunction of the Schrödinger equation by considering how atoms combine to form molecules. Through the interactions of AOs, it explains bond formation in terms of the overlap of wavefunctions and the pairing of electrons. VBT states that a chemical bond forms when AOs of two atoms overlap, allowing electrons to be shared between them. The greater the overlap, the stronger the bond. The overlapping orbitals must have compatible symmetry, similar energy levels, and opposite spins. There are two major types of orbital overlapping: sigma (σ) bonds via head-on overlap of AOs along the internuclear

axis and pi (π) bonds through side-by-side overlap of p AOs perpendicular to the internuclear axis. VBT also introduced orbital hybridization to explain molecular geometry and resonance to justify bonding that cannot be adequately described by a single Lewis structure.

The building block of the many-electron wavefunction Ψ in VBT is the so-called Heitler–London–Pauling–Slater (HLSP) function [4], also called VB function, which refers to the many-electron wavefunction used in VBT to describe covalent bond formation between two atoms. Using the H_2 molecule as an example, let $\phi_A(1)$ and $\phi_B(2)$ represent the AOs of hydrogen atoms A and B, respectively, where $\phi_A(1)$ is the 1s AO of atom A for electron 1, and $\phi_B(2)$ is the 1s AO of atom B for electron 2. The spatial part of the wavefunction is constructed as a linear combination of product states, ensuring proper symmetry under electron exchange,

$$\Psi_{\text{spatial}} = \frac{1}{\sqrt{2 \pm S}}\left[\phi_A(1)\phi_B(2) \pm \phi_A(2)\phi_B(1)\right], \tag{1.3}$$

where the "+" sign corresponds to the symmetric spatial wavefunction (bonding orbital), the "−" sign corresponds to the antisymmetric spatial wavefunction (antibonding orbital), and S is the overlap integral between two nonorthogonal AOs,

$$S = \int \phi_A(\mathbf{r})\phi_B(\mathbf{r})d\mathbf{r}. \tag{1.4}$$

Since electrons are fermions, the many-electron wavefunction (spatial × spin) must be antisymmetric under spin exchange between spin-up (α) and spin-down (β) electrons. Therefore, we have the spin part of the total wavefunction,

$$\Psi_{\text{spin}} = \frac{1}{\sqrt{2}}\left[(\alpha(1)\beta(2) \mp \beta(1)\alpha(2))\right]. \tag{1.5}$$

The HLSP function Ψ_{HLSP} is the product of spatial and spin parts,

$$\Psi_{\text{HLSP}} = \Psi_{\text{spatial}} \ * \ \Psi_{\text{spin}}. \tag{1.6}$$

In general, in VBT, the many-electron wavefunction Ψ of a molecule can be expressed in terms of a linear combination of HLSP functions, as

$$\Psi = \sum\nolimits_K C_K \Psi^K_{\text{HLSP}}, \tag{1.7}$$

where Ψ^K_{HLSP} is a VB function (e.g., HLSP function) corresponding to a specific Lewis structure, and C_K is its corresponding coefficient. A general HLSP function can be written as

$$\Psi^K_{\text{HLSP}} = \widehat{A}\,\Omega_K\,\Theta_K, \tag{1.8}$$

where $\widehat{A}$ is the antisymmetrization operator and Ω_K is a direct product of occupied spatial AOs $\{\phi_{K_i}\}$,

$$\Omega_K = \phi_{K_1}(1)\phi_{K_2}(2)\cdots\phi_{K_N}(N), \tag{1.9}$$

and the spin contribution Θ_K is

$$\Theta_K = \prod_{(ij)} \frac{1}{\sqrt{2}} [\alpha(i)\beta(j) - \beta(i)\alpha(j)] \prod_k \alpha(k), \tag{1.10}$$

where (ij) runs over all n covalent bonds and k runs over all unpaired electrons, which implies that an HLSP function is expanded as a linear combination of 2^n Slater determinants.

With the above approximate total wave function Ψ, one can solve the generalized eigenvalue equation,

$$\mathbf{HC} = \mathbf{SC}\boldsymbol{\varepsilon}, \tag{1.11}$$

where $\mathbf{H}$ and $\mathbf{S}$ are Hamiltonian and overlap matrices constructed in the basis of HLSP functions, respectively, $\mathbf{C}$ and $\boldsymbol{\varepsilon}$ are eigenvectors and eigenvalues. This equation must be numerically solved self-consistently.

The key advantage of VBT is that each HLSP function exactly corresponds to a classical Lewis structure, and thus it provides unambiguous and intuitive insights into the nature of chemical bonding and reactivity mechanisms. Additionally, Pauling's hybridization theory successfully explains molecular geometry and resonance structures. On the other hand, VBT cannot easily explain delocalized electron systems, does not account well for excited states, and becomes mathematically complex for larger molecules. Recent developments in VBT have resolved some of these issues with methods like generalized valence bond theory [27], ab initio VBT [4], and block-localized wavefunction theory [28].

1.3.2 Molecular Orbital Theory

MOT is the second electronic structure theory to approximately solve the Schrödinger equation. Developed in the 1930s by Robert Mulliken [29] and Friedrich Hund [30, 31], and later by many others, MOT introduces the concept of MOs, which are formed from the linear combination of atomic orbitals (LCAOs). Unlike VBT, which focuses on using AOs to form localized covalent bonds, MOT emphasizes the delocalized nature of electrons in MOs. This delocalization enables MOT to describe a broader range of chemical phenomena, from conjugated systems and aromaticity to bonding in metals and coordination complexes.

To form an approximate many-electron wavefunction Ψ for Eq. (1.1), MOT starts with the Born–Oppenheimer approximation to separate the motion of electrons from that of atomic nuclei within a molecule because atomic nuclei are much heavier than electrons and then uses the LCAO approximation to generate MOs,

$$\psi_i = a \sum\nolimits_j c_{ij} \phi_j \tag{1.12}$$

where ψ_i are MOs, ϕ_j AOs, c_{ij} linear coefficients, and a the normalization constant. Since electrons are fermions, the many-electron wavefunction represented by MOs should satisfy the antisymmetric condition, which is done through the Slater determinant,

$$\Psi(\mathbf{x_1}, \mathbf{x_2}, \cdots, \mathbf{x_N}) = \frac{1}{\sqrt{N!}} \begin{vmatrix} \psi_1(\mathbf{x_1}) & \psi_2(\mathbf{x_1}) & \cdots & \psi_N(\mathbf{x_1}) \\ \psi_1(\mathbf{x_2}) & \psi_2(\mathbf{x_2}) & \cdots & \psi_N(\mathbf{x_2}) \\ \vdots & \vdots & \ddots & \vdots \\ \psi_1(\mathbf{x_N}) & \psi_2(\mathbf{x_N}) & \cdots & \psi_N(\mathbf{x_N}) \end{vmatrix}, \tag{1.13}$$

where $\mathbf{x}$ denotes the position and spin coordinate of a single electron for an N-electron system. If the many-electron wavefunction in Eq. (1.1) is expressed by the above single Slater determinant, this method is called the Hartree–Fock (HF) method. In this case, plugging Eq. (1.13) into Eq. (1.2) to variationally optimize all linear coefficients in Eq. (1.12), one obtains the so-called Hartree–Fock–Roothaan equation with the basis set $\{\phi_i\}$,

$$\mathbf{Fc} = \mathbf{Sc}\boldsymbol{\varepsilon}, \tag{1.14}$$

where $\mathbf{F}$ is the Fock matrix, $\mathbf{S}$ is the overlap matrix of the basis functions, $\mathbf{c}$ is the coefficient matrix, and $\boldsymbol{\varepsilon}$ is the diagonal matrix of orbital energies. In the case of an orthonormalized basis set, the overlap matrix, $\mathbf{S}$, reduces to the identity matrix. Same as Eq. (1.11) in VBT, Eq. (1.14) should be solved numerically in the self-consistent-field (SCF) manner. The obtained MOs are occupied from the lowest orbital energy, each by two antiparallel electrons, forming the ground state of the system.

Since the HF method uses only one Slater determinant in approximating the many-electron wavefunction, it only includes the static correlation stemming from the exchange effect among spin-parallel electrons. The configuration interaction (CI) method goes beyond the HF method by including the dynamic correlation effect from spin-antiparallel electrons. It does so by expressing the many-electron wavefunction as a linear combination of multiple Slater determinants,

$$\Psi_{\mathrm{CI}} = c_0 \Psi_0 + \sum\nolimits_i c_i \Psi_i + \sum\nolimits_{i<j} c_{ij} \Psi_{ij} + \cdots \tag{1.15}$$

where Ψ_0 is the HF ground-state determinant; $\Psi_i, \Psi_{ij}, \cdots$, are excited determinants obtained by promoting one, two, or more electrons from occupied MOs to unoccupied (virtual) orbitals; and $c_0, c_i, c_{ij}, \cdots$, are the coefficients determined variationally. If only single excitation is considered, that is, the right-hand side of Eq. (1.15) is truncated at the second term, we have CIS (CI singles); if two electrons are promoted (i.e., Eq. (1.15) is truncated up to the third term), we have CISD (CI singles and doubles); if it includes all possible excitations in Eq. (1.15), the full CI (FCI) method is obtained. FCI represents the most accurate results that can be obtained by MOT. Because FCI is exceedingly costly in computational expenses, it is limited only to small systems. CI methods improve the accuracy of molecular energy calculations, capture dynamic electron correlation effects, and provide a systematic way to improve results.

Figure 1.3 depicts the relationship between HF and FCI methods. Other multi-determinant approaches are available in the literature, such as coupled cluster theory, complete active space SCF theory, and multi-reference CI. Also included in Figure 1.3 is the series of perturbation theories, such as MP2 (second-order Møller–Plesset perturbation theory) and CASPT2 (complete active space second-order

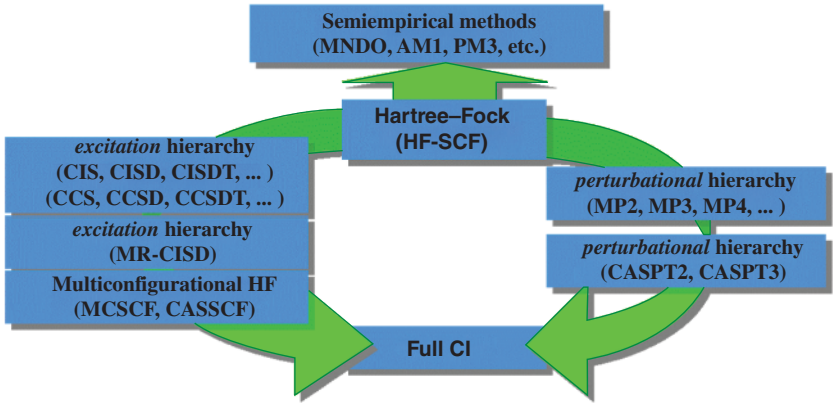

Figure 1.3 Available approaches in MOT.

perturbation theory). On top of the figure are semiempirical approaches that simplify the ab initio wavefunction theory by (i) employing one Slater determinant, (ii) focusing only on valence electrons, and (iii) incorporating experimental parameters to neglect or approximate certain two-electron integrals. These simplifications significantly reduce computational costs and thus make them suitable for treating large systems, such as biomolecules and polymers.

1.3.3 Concepts from Orbital-based Theories

The two frameworks of orbital-based theories, VBT and MOT, not only provide practical pathways to approximately solve the Schrödinger equation numerically for many-electron systems but also offer insights and understanding about various chemical concepts [32, 33].

In VBT, how AOs of individual atoms overlap to form chemical bonds is the focus [32]. A chemical bond forms when the AOs of two atoms overlap, resulting in a region of shared electron density between the two nuclei. Greater overlapping leads to stronger bonding and lower potential energy of the molecular system. When the two AOs are overlapped head-on, a sigma (σ) bond is formed. When they overlap side-by-side, a pi (π) bond is formed, which often accompanies a sigma bond in double and triple bonds.

The hybridization concept introduced by Linus Pauling explains how AOs can combine to form new hybrid AOs with different shapes, such as sp, sp^2, sp^3, and sp^3d^2, which can be used to predict bond angles and molecular geometry, for example, tetrahedral and trigonal planar.

When a single VB structure cannot fully represent the true electronic structure of a molecule, such as benzene, the concept of resonance is introduced by Pauling and Hund to describe the situation. In this case, multiple VB structures, called *resonance structures*, contribute to the overall bonding and properties of the molecule. The actual molecule is considered a *resonance hybrid*, which is a weighted average of these resonance structures. First proposed by Shaik et al. [34, 35], a *charge-shift*

(CS) bond is a type of chemical bond where the stability arises not primarily from covalent or ionic character but from resonance between ionic structures. This phenomenon occurs when the bond energy cannot be fully explained by the simple combination of covalent and ionic bonding contributions. The first example of such a CS bond is the diatomic molecule F_2.

VBT emphasizes localization of chemical bonding, where electrons are shared between specific pairs of atoms. Nevertheless, it can also provide qualitative understanding about conjugation, hyperconjugation, and aromaticity [32]. Conjugation occurs when a molecule has alternating single and multiple bonds (e.g., C═C—C═C), allowing π-electrons to delocalize over adjacent atoms. In VBT, conjugation is explained by the overlap of adjacent p-orbitals on sp^2-hybridized atoms. This overlap creates a π-electron cloud that extends over multiple atoms, leading to electron delocalization and overall decreased energy. Hyperconjugation involves the delocalization of electrons from a σ-bond (usually C—H or C—C) into an adjacent empty or partially filled p-orbital or π-system, whereas aromaticity refers to the exceptional stability of cyclic, planar molecules with delocalized π-electrons, governed by Hückel's rule ($4n + 2$ π-electrons). With overlapping between σ- or π-bonds, VBT can provide qualitative descriptions about conjugation, hyperconjugation, and aromaticity, but its understanding is often less quantitative than MOT.

MOT provides a comprehensive understanding of chemical bonding, electronic structure, and molecular properties [33, 36–38]. Since an MO is formed by the LCAOs from different atoms in a molecule, electrons in a molecule occupying such MOs are usually delocalized over the entire molecule rather than being associated with a single atom or localized between a pair of atoms. Also, MOs, either head-on (σ overlap) or side-on (π overlap), can be *bonding* (in-phase overlap, lowering energy, e.g., σ or π) or *antibonding* (out-of-phase overlap, raising energy, e.g., σ* or π*) or *nonbonding* (no overlap, no change in energy). These different bonding natures of MOs can be represented by the MO diagram, as shown in Figure 1.4 for O_2 as an example. It elucidates the relative energy of MOs with respect to

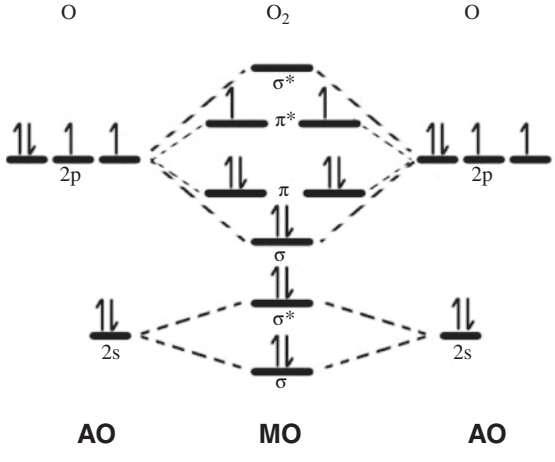

Figure 1.4 The MO diagram of the oxygen molecule. Only valence orbitals are shown.

those of AOs. Electrons fill MOs in the diagram according to the *Aufbau principle* (electrons occupy MOs in order of increasing energy), *Pauli exclusion principle* (each MO can only occupy two antiparallel electrons), and *Hund's rule* (when electrons occupy degenerate MOs, they will first fill each orbital singly with parallel spins before pairing up). Using the diagram, one can evaluate bond orders, determine paramagnetic and diamagnetic properties, and quantitatively describe conjugation, hyperconjugation, and aromaticity.

Even though localization and hybridization are concepts from VBT, it can be integrated with MOT to explain molecular geometry and bonding through, for example, the *natural bond orbital* analysis [39, 40]. Localized molecular orbitals (LMOs) are obtained through the unitary transformation of the conventional, delocalized MOs. LMOs are spatially concentrated in specific regions of a molecule and thus provide an intuitive picture of bonding that resembles the traditional Lewis structure, where bonds are localized between pairs of atoms and lone pairs are confined to specific atoms.

Molecules have symmetry, so do AOs and MOs. AOs that have the same symmetry with respect to a molecule's symmetry elements can mix and form MOs, whereas those with different symmetries do not interact, due to orthogonality. LCAO preserves the symmetry property of the molecule, leading to the *orbital symmetry conservation principle* in MOT [38]. As a result, MOs inheriting the symmetry of a molecule can be classified as σ, π, δ, or with symmetry labels such as a_1 and b_2. Based on this principle for chemical reactions, Woodward and Hoffmann proposed a set of rules, called the *Woodward–Hoffmann rules* [37, 38], to predict the outcome of pericyclic reactions.

The frontier molecular orbital (FMO) theory proposed by Kenichi Fukui is a conceptual framework in MOT to explain and predict chemical reactivity and selectivity [36, 41, 42]. It focuses on the interaction between the highest-occupied MO and the lowest-unoccupied molecular orbital of the reactants. These orbitals, referred to as the "frontier orbitals," are most important in governing the reactivity of molecules. Because of this work, Fukui shared the 1981 Nobel Prize in Chemistry with Roald Hoffmann for his contribution to establishing the Woodward–Hoffmann rules.

1.4 Density Functional Theory

DFT [9] has been the workhorse in the past few decades as the most widely used computational method to simulate the electronic structure of molecules and condensed matter alike [43]. It has become a cornerstone of materials science, chemistry, and condensed matter physics due to its balance of remarkable accuracy and computational efficiency. At its core, unlike VBT and MOT, DFT avoids directly solving the Schrödinger equation, Eq. (1.1), with an approximate many-electron wavefunction Ψ. Instead, it rewrites Eq. (1.2) as

$$E = E[\rho], \tag{1.16}$$

where $\rho \equiv \rho(\mathbf{r})$ stands for the electron density of a many-electron system in the ground state, which is a function of only three spatial coordinates and is normalized to N,

$$\int \rho(\mathbf{r}) d\mathbf{r} = N, \tag{1.17}$$

where N is the total number of electrons in the system. This electron density $\rho(\mathbf{r})$ can be obtained experimentally from X-ray crystallography. It can also be obtained from wavefunction theory from the N-body wavefunction, $\Psi(\mathbf{r}_1, \mathbf{r}_2, \ldots, \mathbf{r}_N)$,

$$\rho(\mathbf{r}) = N \iint \cdots \int |\Psi(\mathbf{r}, \mathbf{r_2}, \ldots, \mathbf{r_N})|^2 \, \mathrm{d}\mathbf{r_2} \, \mathrm{d}\mathbf{r}_3 \cdots \mathrm{d}\mathbf{r}_N, \tag{1.18}$$

or MOs $\{\psi_i(\mathbf{r})\}$,

$$\rho(\mathbf{r}) = \sum_{i=1}^{\mathrm{occ}} |\psi_i(\mathbf{r})|^2, \tag{1.19}$$

where the sum runs over all occupied MOs in the single-particle approximation, such as in Hartree–Fock theory.

The idea of describing an electronic system by its density goes back to the Thomas–Fermi model developed separately by Thomas [44] and Fermi [45]. In these early works, the electron density was used as a central variable. However, the notation was not entirely standardized then. Many authors used symbols like $n(\mathbf{r})$ or $\rho(\mathbf{r})$ interchangeably to denote the electron density. To the best of the author's knowledge, it was Dirac's 1930 paper "Note on Exchange Phenomena in the Thomas Atom" [46] that derived an expression for the exchange energy of an electron gas and formulated it in terms of the local electron density, denoted by $\rho(\mathbf{r})$. This paper can be credited as the first influential instance where the symbol $\rho(\mathbf{r})$ was used explicitly to represent the electron density.

Equation (1.16) suggests that the total energy of the system is a functional of the electron density, as opposed to Eq. (1.2), where the total energy is a functional of the many-electron wavefunction,

$$E \equiv E\left[\Psi(\mathbf{r_1}, \mathbf{r_2}, \ldots, \mathbf{r_N})\right]. \tag{1.20}$$

This reformulation of Eq. (1.16) is based on the two Hohenberg–Kohn theorems [8]. The first one states that there is a one-to-one mapping between the electron density $\rho(\mathbf{r})$ and the external potential $v_{\mathrm{ext}}(\mathbf{r})$ in the ground state. This suggests that all ground state properties of the system are functionals of the electron density, including the total energy,

$$E[\rho] = F[\rho] + \int \rho(\mathbf{r}) v_{\mathrm{ext}}(\mathbf{r}) \mathrm{d}\mathbf{r}, \tag{1.21}$$

where $F[\rho]$ is the universal density functional. The second theorem asserts that the correct ground-state electron density should minimize the total energy functional, thus providing a variational principle for Eq. (1.21) and yielding the following Euler equation,

$$\mu = \frac{\delta E[\rho]}{\delta \rho(\mathbf{r})} = \frac{\delta F[\rho]}{\delta \rho(\mathbf{r})} + \upsilon_{\text{ext}}(\mathbf{r}), \tag{1.22}$$

where μ is the chemical potential and $\delta/\delta\rho(\mathbf{r})$ is the functional derivative with respect to the electron density [9].

According to these theorems, in principle, any energetic component of the total electronic energy can be rigorously expressed by a density functional, but in practice it is impossible to do so. In DFT, a conventional partition of the total electronic energy is the following,

$$E[\rho] = T_S[\rho] + V_{ne}[\rho] + J[\rho] + E_{xc}[\rho], \tag{1.23}$$

where T_S is the noninteracting total kinetic energy, V_{ne} the electron–nucleus attraction, J the electron–electron Coulombic repulsion, and E_{xc} the exchange–correlation energy, which captures the quantum mechanical effects of electron exchange and correlation. Note that when calculating the total energy, one should add the electrostatic repulsion among nuclei, V_{nn}. Among the four components in Eq. (1.23), only two terms are known to have an explicit expression in terms of the electron density. The first is $V_{ne}[\rho]$, which is the second term at the right-hand side of Eq. (1.21), and the other is the classical electron–electron Coulombic repulsion J$[\rho]$,

$$J[\rho] = \frac{1}{2}\iint \frac{\rho(\mathbf{r})\rho(\mathbf{r}')}{|\mathbf{r} - \mathbf{r}'|} \boldsymbol{d}\mathbf{r}\boldsymbol{d}\mathbf{r}'. \tag{1.24}$$

For $T_S[\rho]$ and $E_{xc}[\rho]$, their exact expression in terms of the electron density is unknown.

To overcome this difficulty, Kohn and Sham [47] introduced a fictitious system of noninteracting electrons moving in the so-called Kohn–Sham orbitals $\{\psi_i(\mathbf{r})\}$ with an effective potential $\upsilon_{eff}(\mathbf{r})$, so the same ground-state electron density $\rho(\mathbf{r})$ as the interacting system is reproduced

$$\rho(\mathbf{r}) = \sum_{i=1}^{N} |\psi_i(\mathbf{r})|^2, \tag{1.25}$$

the noninteracting total kinetic energy is expressed as

$$T_S[\rho] = -\frac{1}{2}\sum_{i=1}^{N} \int \psi_i(\mathbf{r}) \nabla^2 \psi_i(\mathbf{r}) \mathrm{d}\mathbf{r}, \tag{1.26}$$

and then the Kohn–Sham equation is obtained as,

$$\left(-\frac{1}{2}\nabla^2 + \upsilon_{eff}(\mathbf{r})\right)\psi_i(\mathbf{r}) = \epsilon_i \psi_i(\mathbf{r}), \tag{1.27}$$

where the effective Kohn–Sham potential is composed of several terms,

$$\upsilon_{eff}(\mathbf{r}) = \upsilon_{ext}(\mathbf{r}) + \upsilon_J(\mathbf{r}) + \upsilon_{xc}(\mathbf{r}), \tag{1.28}$$

with the classical Coulombic potential

$$v_J(\mathbf{r}) = \int \frac{\rho(\mathbf{r}')}{|\boldsymbol{r} - \mathbf{r}'|} d\mathbf{r}', \tag{1.29}$$

and the exchange–correlation potential

$$v_{xc}(\mathbf{r}) = \frac{\delta E_{xc}[\rho]}{\delta \rho(\mathbf{r})}. \tag{1.30}$$

In the Kohn–Sham scheme, the total kinetic energy is obtained by Eq. (1.26), so there is only one unknown left in Eq. (1.23) to approximate, which is the exchange–correlation energy density functional $E_{xc}[\rho]$.

The development and history of DFT are closely tied to the search for better exchange–correlation functionals because $E_{xc}[\rho]$ is the key approximation in the Kohn–Sham equation that determines its accuracy and applicability. The local density approximation (LDA) was the first form proposed, and it is the simplest exchange–correlation functional. It assumes that the exchange–correlation energy at any point in space depends only on the local electron density at that point,

$$E_{xc}^{\mathrm{LDA}} = \int \rho(\mathbf{r}) e_{xc}(\rho(\mathbf{r})) d\mathbf{r}, \tag{1.31}$$

where $e_{xc}(\rho)$ is the exchange–correlation energy per particle. LDA works surprisingly well for systems with slowly varying electron densities (e.g., simple metals) but fails for systems with strong inhomogeneities (e.g., atoms, molecules, surfaces). To address the limitations of LDA, the generalized gradient approximation (GGA) [48] was developed, including not only the local electron density but also its gradient,

$$E_{xc}^{\mathrm{GGA}} = \int \rho(\mathbf{r}) e_{xc}(\rho(\mathbf{r}), \nabla\rho(\mathbf{r})) d\mathbf{r}. \tag{1.32}$$

GGA functionals, such as B88 (Becke 88) [49], Lee–Yang–Parr (LYP) [50], and Perdew–Burke–Ernzerhof [51], significantly improved the accuracy of DFT for molecular systems, bond energies, and structural properties. Another popular category is the hybrid functional, such as B3LYP (Becke 3-parameter Lee-Yang-Parr), mix a portion of exact exchange from Hartree–Fock theory with GGA exchange and correlation,

$$E_{xc}^{\mathrm{Hybrid}} = aE_x^{\mathrm{HF}} + (1-a)E_x^{\mathrm{GGA}} + E_c^{\mathrm{GGA}}, \tag{1.33}$$

where E_x^{HF} is the exact exchange energy from Hartree–Fock theory.

Other kinds of approximate exchange–correlation functionals in DFT are (i) meta-GGA functionals, such as Tao–Perdew–Staroverov–Scuseria [52] and Strongly Constrained and Appropriately Normed [53], which go beyond GGA by including higher-order derivatives of the electron density (e.g., the kinetic energy density), and (ii) range-separated hybrid and double hybrid functionals [54], which further refine the treatment of exchange and correlation energies by incorporating long-range corrections and perturbative correlation, respectively.

Unlike ab initio wavefunction theory methods in Figure 1.3, where a clear pathway is available to systematically improve the accuracy, DFT does not have such a route.

Figure 1.5 The Jacob's ladder in DFT (Generated with AI using DALL·E—OpenAI).

Still, the Jacob's ladder metaphor in DFT, shown in Figure 1.5, represents the hierarchy of increasingly accurate density functionals. This "ladder" metaphor, introduced by John P. Perdew, compares functional development to climbing a ladder toward the "heaven" of chemical accuracy. Each rung of the ladder corresponds to a level of approximation, with higher rungs providing greater accuracy but also increasing computational cost. It serves as a framework to understand the tradeoff between accuracy and computational cost in DFT, guiding researchers in choosing the appropriate functional for their systems.

DFT has become immensely popular over the last few decades due to its unique combination of accuracy, versatility, and computational efficiency. While DFT is powerful and widely used, its limitations arise primarily from approximations in the exchange–correlation functional and its inability to handle specific phenomena like strong correlation, excited states, or van der Waals interactions. Manifested by, for example, the self-interaction error [55], it overestimates electron delocalization, leading to incorrect prediction of properties like band gaps, dissociation energies, and ionization potentials. On the other hand, it underestimates electron localization, causing a poor description of charge transfer, oxidation states, spin states, or

electronic configurations of localized systems such as transition metal complexes. These errors arise because DFT functionals do not fully capture the complex exchange and correlation effects. Recent developments, such as double hybrid functionals (e.g., B2PLYP), combine a portion of exact exchange with a perturbative treatment of correlation, providing a more balanced description of delocalized and localized states. Additionally, ML techniques are being used to develop new functionals that better capture the complexities of electron delocalization and localization [56–58].

1.5 Scope of This Book

We want insight, not just numbers [20]. Any electronic structure theory should provide a new understanding of traditional chemical concepts. As highlighted in Section 1.3, VBT did that with the insight into chemical bonding, and MOT provided the FMO theory, orbital symmetry conservation principle, and Woodward–Hoffmann rules. They are both orbital-based. In DFT, electron density is the basic variable. To the best of the author's knowledge, there is no systematic work to present all conceptual frameworks to harness chemical understanding using density-based ideas [59–61]. Conceptual DFT (CDFT) [9, 62–65] is the first effort in DFT to analyze chemical reactivity in terms of global and local descriptors such as electronegativity, hardness, and electrophilicity. Other efforts such as quantum theory of atoms in molecules (QTAIM) [66], electron localization function (ELF) [67], and noncovalent interaction (NCI) [68, 69] analyses are also available in the literature. However, their scope is limited, and controversies are abundant. The purpose of this book is to fill the knowledge gap by providing a systematic overview of how to employ density-based ideas to harvest chemical insights, including covalent bonding, weak interactions, conformational stability, acidity/basicity, electrophilicity, nucleophilicity, aromaticity, stereoselectivity, and catalysis, with density-based descriptors.

In what follows, in Part I of this book, we will present the four density-based frameworks, including CDFT (Chapter 2), density-associated quantities (Chapter 3), information-theoretic approach (Chapter 4), and orbital-free DFT (Chapter 5), and the interrelationships among these frameworks as well as a few recent developments (Chapter 6).

In Part II, applications of these four frameworks to real chemical problems are discussed, including covalent and noncovalent interactions (Chapter 7), cooperativity and frustration (Chapter 8), principle of chirality hierarchy and homochirality (Chapter 9), electrophilicity and nucleophilicity (Chapter 10), steric effect and stereoselectivity (Chapter 11), acidity and basicity (Chapter 12), aromaticity and antiaromaticity (Chapter 13), excited states (Chapter 14), catalysis (Chapter 15), and miscellaneous applications (Chapter 16).

In Part III, based on the ideas from this book, in the final two chapters (Chapters 17 and 18), we provide perspectives on how chemical understanding is, in general, obtained with chemical concepts (Chapter 17) and how to expand the territory of chemical reactivity theory by harvesting chemical understanding with ML and quantum computing (Chapter 18).

References

1 Heitler W, London F. Wechselwirkung neutraler Atome und homopolare Bindung nach der Quantenmechanik. Z Phys. 1927 Jun;44(6–7):455–72.
2 Gerratt J, Cooper DL, Karadakov PB, Raimondi M. Modern valence bond theory. Chem Soc Rev. 1997;26(2):87.
3 Shaik S, Hiberty PC. Valence bond theory, its history, fundamentals, and applications: a primer. In: Lipkowitz KB, Larter R, Cundari TR, editors. Reviews in Computational Chemistry. Wiley; 2004. pp. 1–100.
4 Zhou C, Wu X, Ying F, Wu W. Ab initio valence bond theory for strongly correlated systems. J Chem Theory Comput. 2025 Jul 8;21(13):6243–57.
5 Roothaan CCJ. New developments in molecular orbital theory. Rev Mod Phys. 1951 Apr 1;23(2):69–89.
6 Hehre WJ. Ab initio molecular orbital theory. Acc Chem Res. 1976 Nov 1;9(11): 399–406.
7 Dewar MJS. A molecular orbital theory of organic chemistry. I. General principles. J Am Chem Soc. 1952;74(13):3341–5.
8 Hohenberg P, Kohn W. Inhomogeneous electron gas. Phys Rev. 1964 Nov 9; 136(3B):B864–71.
9 Parr RG, Weitao Y. Density-Functional Theory of Atoms and Molecules. Oxford University Press; 1995.
10 Cohen AJ, Mori-Sánchez P, Yang W. Challenges for density functional theory. Chem Rev. 2012 Jan 11;112(1):289–320.
11 Tozzini V. Multiscale modeling of proteins. Acc Chem Res. 2010 Feb 16;43(2): 220–30.
12 Horstemeyer MF. Multiscale modeling: a review. In: Leszczynski J, Shukla MK, editors. Practical aspects of computational chemistry. Dordrecht: Springer Netherlands; 2010. pp. 87–135.
13 Mjolsness E, DeCoste D. Machine learning for science: state of the art and future prospects. Science. 2001 Sep 14;293(5537):2051–5.
14 Rupp M, Tkatchenko A, Müller K-R, von Lilienfeld OA. Fast and accurate modeling of molecular atomization energies with machine learning. Phys Rev Lett. 2012 Feb 3;108(5):058301.
15 LeCun Y, Bengio Y, Hinton G. Deep learning. Nature. 2015 May 28;521 (7553):436–44.
16 Huang B, von Lilienfeld OA. Ab initio machine learning in chemical compound space. Chem Rev. 2021 Aug 25;121(16):10001–36.
17 Keith JA, Vassilev-Galindo V, Cheng B, Chmiela S, Gastegger M, Müller K-R, et al. Combining machine learning and computational chemistry for predictive insights into chemical systems. Chem Rev. 2021 Aug 25;121(16):9816–72.
18 Kulichenko M, Nebgen B, Lubbers N, Smith JS, Barros K, Allen AEA, et al. Data generation for machine learning interatomic potentials and beyond. Chem Rev. 2024 Nov 21;124:13681–714.

19 Meuwly M. Machine learning for chemical reactions. Chem Rev. 2021 Aug 25;121(16):10218–39.

20 Liu S. Harvesting chemical understanding with machine learning and quantum computers. ACS Phys Chem Au. 2024 Mar 27;4(2):135–42.

21 Liu S. Exploring Chemical Concepts Through Theory and Computation. Wiley; 2024.

22 Agranat I. Aromaticity – a theoretical notion. Struct Chem. 2024 Jun;35(3):715–20.

23 Neese F, Atanasov M, Bistoni G, Maganas D, Ye S. Chemistry and quantum mechanics in 2019: give us insight and numbers. J Am Chem Soc. 2019 Feb 20;141(7):2814–24.

24 Vennelakanti V, Nazemi A, Mehmood R, Steeves AH, Kulik HJ. Harder, better, faster, stronger: large-scale QM and QM/MM for predictive modeling in enzymes and proteins. Curr Opin Struct Biol. 2022 Feb;72:9–17.

25 Tzeliou CE, Mermigki MA, Tzeli D. Review on the QM/MM methodologies and their application to metalloproteins. Molecules. 2022 Apr 20;27(9):2660.

26 Pauling L. The nature of the chemical bond—1992. J Chem Educ. 1992 Jul;69(7):519.

27 Dunning TH, Xu LT, Takeshita TY, Lindquist BA. Insights into the electronic structure of molecules from generalized valence bond theory. J Phys Chem A. 2016 Mar 24;120(11):1763–78.

28 Mo Y, Song L, Lin Y. Block-localized wavefunction (BLW) method at the density functional theory (DFT) level. J Phys Chem A. 2007 Aug 30;111(34):8291–301.

29 Mulliken RS. Spectroscopy, molecular orbitals, and chemical bonding. Science. 1967 Jul 7;157(3784):13–24.

30 Hund F. Zur deutung der molekelspektren. IV. Z Phys. 1928 Nov;51(11–12): 759–95.

31 Murrell JN. The origins and later developments of molecular orbital theory. Int J Quantum Chem. 2012 Sep 5;112(17):2875–9.

32 Zhou C, Ying F, Wu W. Chemical concepts from *ab initio* valence bond theory. In: Liu S, editor. Exploring Chemical Concepts Through Theory and Computation. Wiley; 2024. pp. 23–42.

33 Long Gu F, Yu J, Yang W. Chemical concepts from molecular orbital theory. In: Liu S, editor. Exploring Chemical Concepts Through Theory and Computation. Wiley; 2024. pp. 1–22.

34 Shaik S, Danovich D, Wu W, Hiberty PC. Charge-shift bonding and its manifestations in chemistry. Nat Chem. 2009 Sep;1(6):443–9.

35 Shaik S, Danovich D, Galbraith JM, Braïda B, Wu W, Hiberty PC. Charge-shift bonding: a new and unique form of bonding. Angew Chem. 2020 Jan 13;132(3):996–1013.

36 Fukui K. Role of frontier orbitals in chemical reactions. Science. 1982 Nov 19;218(4574):747–54.

37 Geerlings P, Ayers PW, Toro-Labbé A, Chattaraj PK, De Proft F. The Woodward-Hoffmann rules reinterpreted by conceptual density functional theory. Acc Chem Res. 2012 May 15;45(5):683–95.

38 Woodward RB, Hoffmann R. The conservation of orbital symmetry. Angew Chem Int Ed. 1969 Nov;8(11):781–853.

39 Reed AE, Weinhold F. Natural localized molecular orbitals. J Chem Phys. 1985 Aug 15;83(4):1736–40.

40 Glendening ED, Landis CR, Weinhold F. Natural bond orbital methods. WIREs Comput Mol Sci. 2012 Jan;2(1):1–42.

41 Yang W, Parr RG, Pucci R. Electron density, Kohn–Sham frontier orbitals, and Fukui functions. J Chem Phys. 1984;81(6):2862.

42 Huang Y, Rong C, Zhang R, Liu S. Evaluating frontier orbital energy and HOMO/LUMO gap with descriptors from density functional reactivity theory. J Mol Model. 2017 Jan;23(1):3.

43 Teale AM, Helgaker T, Savin A, Adamo C, Aradi B, Arbuznikov AV, et al. DFT exchange: sharing perspectives on the workhorse of quantum chemistry and materials science. Phys Chem Chem Phys. 2022 Dec 7;24(47):28700–81.

44 Thomas LH. The calculation of atomic fields. Math Proc Camb Phil Soc. 1927;23:542–8.

45 Fermi E. Eine statistische methode zur bestimmung einiger eigenschaften des atoms und ihre anwendung auf die theorie des periodischen systems der elemente. Z Phys. 1928 Jan;48(1–2):73–9.

46 Dirac PAM. Note on exchange phenomena in the thomas atom. Math Proc Camb Phil Soc. 1930 Jul;26(03):376.

47 Kohn W, Sham LJ. Self-consistent equations including exchange and correlation effects. Phys Rev. 1965 Nov 15; 140(4A):A1133–8.

48 Burke K, Perdew JP, Ernzerhof M. Why the generalized gradient approximation works and how to go beyond it. Int J Quantum Chem. 1997 Jan 1;61(2):287–93.

49 Becke AD. A multicenter numerical integration scheme for polyatomic molecules. J Chem Phys. 1988;88(4):2547.

50 Lee C, Yang W, Parr RG. Development of the Colle-Salvetti correlation-energy formula into a functional of the electron density. Phys Rev B Condens Matter. 1988 Jan 15;37(2):785–9.

51 Perdew JP, Burke K, Ernzerhof M. Generalized gradient approximation made simple. Phys Rev Lett. 1996 Oct 28;77(18):3865–8.

52 Tao J, Perdew JP, Staroverov VN, Scuseria GE. Climbing the density functional ladder: nonempirical meta-generalized gradient approximation designed for molecules and solids. Phys Rev Lett. 2003 Oct 3;91(14):146401.

53 Sun J, Ruzsinszky A, Perdew JP. Strongly constrained and appropriately normed semilocal density functional. Phys Rev Lett. 2015 Jul 17;115(3):036402.

54 Brémond É, Pérez-Jiménez ÁJ, Sancho-García JC, Adamo C. Range-separated hybrid and double-hybrid density functionals: a quest for the determination of the range-separation parameter. J Chem Phys. 2020 Jun 28;152(24):244124.

55 Cohen AJ, Mori-Sánchez P, Yang W. Insights into current limitations of density functional theory. Science. 2008 Aug 8;321(5890):792–4.

56 Voss J. Machine learning for accuracy in density functional approximations. J Comput Chem. 2024 Apr 26;45:1829–45.

57 Remme R, Kaczun T, Ebert T, Gehrig CA, Geng D, Gerhartz G, et al. Stable and accurate orbital-free density functional theory powered by machine learning. J Am Chem Soc. 2025 Aug 1; 147(32):28851–9.

58 Kumar S, Jing X, Pask JE, Medford AJ, Suryanarayana P. Kohn-Sham accuracy from orbital-free density functional theory via Δ-machine learning. J Chem Phys. 2023 Dec 28;159(24).

59 Rong C, Zhao D, He X, Liu S. Development and applications of the density-based theory of chemical reactivity. J Phys Chem Lett. 2022 Dec 8;13(48):11191–200.

60 He X, Li M, Rong C, Zhao D, Liu W, Ayers PW, et al. Some recent advances in density-based reactivity theory. J Phys Chem A. 2024 Feb 22;128(7):1183–96.

61 An X, Zhang W, He X, Li M, Rong C, Liu S. Density-based reactivity theory applied to excited states. AAPPS Bull. 2024 Feb 2;34(1):8.

62 Liu S. Conceptual density functional theory and some recent developments. Acta Phys-Chim Sin. 2009;25(3):590–600.

63 Liu S, editor. Conceptual Density Functional Theory: Towards a New Chemical Reactivity Theory. 1st ed. Wiley-VCH GmbH: Wiley; 2022.

64 Geerlings P, De Proft F, Langenaeker W. Conceptual density functional theory. Chem Rev. 2003 May;103(5):1793–873.

65 Geerlings P, Chamorro E, Chattaraj PK, De Proft F, Gázquez JL, Liu S, et al. Conceptual density functional theory: status, prospects, issues. Theor Chem Acc. 2020 Feb;139(2):36.

66 Bader RFW. Atoms in Molecules. Oxford University Press;1989.

67 Savin A, Nesper R, Wengert S, Fässler TF. ELF: the electron localization function. Angew Chem Int Ed. 1997 Sep 17;36(17):1808–32.

68 Johnson ER, Keinan S, Mori-Sánchez P, Contreras-García J, Cohen AJ, Yang W. Revealing noncovalent interactions. J Am Chem Soc. 2010 May 12;132(18):6498–506.

69 Contreras-García J, Johnson ER, Keinan S, Chaudret R, Piquemal J-P, Beratan DN, et al. NCIPLOT: a program for plotting non-covalent interaction regions. J Chem Theory Comput. 2011 Mar 8;7(3):625–32.